Current Biology *18*, 1860–1864, December 9, 2008 ©2008 Elsevier Ltd All rights reserved DOI 10.1016/j.cub.2008.10.026

Report

The Homotetrameric Kinesin-5 KLP61F Preferentially Crosslinks Microtubules into Antiparallel Orientations

Siet M.J.L. van den Wildenberg,[1,4] Li Tao,[2,4] Lukas C. Kapitein,[1,5] Christoph F. Schmidt,[3] Jonathan M. Scholey,[2,*] and Erwin J.G. Peterman[1,*]

[1]Department of Physics and Astronomy and Laser Centre
VU University Amsterdam
1081 HV Amsterdam
The Netherlands

[2]Department of Molecular and Cell Biology
University of California at Davis
Davis, CA 95616
USA

[3]Department of Physics
Georg August University
37077 Göttingen
Germany

Summary

The segregation of genetic material during mitosis is coordinated by the mitotic spindle, whose action depends upon the polarity patterns of its microtubules (MTs) [1, 2]. Homotetrameric mitotic kinesin-5 motors can crosslink and slide adjacent spindle MTs [3–11], but it is unknown whether they or other motors contribute to establishing these MT polarity patterns. Here, we explored whether the *Drosophila* embryo kinesin-5 KLP61F, which plausibly crosslinks both parallel and antiparallel MTs [7, 12], displays a preference for parallel or antiparallel MT orientation. In motility assays, KLP61F was observed to crosslink and slide adjacent MTs, as predicted. Remarkably, KLP61F displayed a 3-fold higher preference for crosslinking MTs in the antiparallel orientation. This polarity preference was observed in the presence of ADP or ATP plus AMPPNP, but not AMPPNP alone, which induces instantaneous rigor binding. Also, a purified motorless tetramer containing the C-terminal tail domains displayed an antiparallel orientation preference, confirming that motor activity is not required. The results suggest that, during morphogenesis of the *Drosophila* embryo mitotic spindle, KLP61F's crosslinking and sliding activities could facilitate the gradual accumulation of KLP61F within antiparallel interpolar MTs at the equator, where the motor could generate force to drive poleward flux and pole-pole separation.

Results and Discussion

KLP61F Can Crosslink and Slide Adjacent Microtubules

By using fluorescence microscopy-based microtubule (MT)-MT sliding assays, we first tested whether purified, full-length KLP61F (Figure 1A, lane 1), like its vertebrate ortholog, Eg5, is able to facilitate MT-MT sliding [4]. To this end, biotinylated Cy-5-labeled MTs were specifically attached to a glass surface. Subsequently, we blocked the surface with the amphiphilic block copolymer Pluronic F108 to prevent nonspecific binding of MTs and KLP61F to the surface. Purified KLP61F and rhodamine-labeled MTs were added together with adenosine triphosphate (ATP). We then acquired time series of images that showed clear movement of rhodamine-labeled MTs over immobilized Cy5-labeled MTs (Figure 1B and Movies S1 and S2, available online). Rhodamine MTs did not land or slide on regions of the surface where no MT was immobilized. This excludes the possibility that MTs were driven by KLP61F directly attached to the glass surface. In most of the recorded events, we observed crosslinked, nonaligned MTs, with a crossover point moving relative to both filaments with an average velocity (± standard deviation) of 11.0 ± 3.1 nm/s (n = 18) (Figures 1C and 1D), which was independent of the crossing angle. Occasionally, as shown in Figures 1B and 1C, the sliding MT rotated into alignment with the immobilized MT, whereupon the two relative velocities of sliding added up to approximately twice the individual velocities, indicating that these MTs all ended up aligned antiparallel [4]. In some of the recorded events, the sliding MT had already been aligned. The average velocity we measured for all aligned, sliding MTs was 26.7 ± 4.5 nm/s (n = 16) (see Figure 1D). These observations suggest that KLP61F can crosslink MTs in either parallel or antiparallel orientation and that it moves with a well-defined velocity along both crosslinked MTs, largely independent of their relative orientation, just like its *Xenopus* ortholog, Eg5 [4]. However, the question remains whether either of these kinesin-5 motors preferentially crosslinks MTs into parallel or antiparallel polarity patterns.

KLP61F Homotetramers Preferentially Crosslink MTs into Antiparallel Bundles

As a prelude to assaying kinesin-5's MT-crosslinking polarity preference, we used standard bundling assays to test the MT-bundling activity of the following constructs: (1) purified full-length KLP61F (a 520 kDa tetrameric holoenzyme), (2) a tetrameric 272 kDa native molecular weight (MW) "stalk" fragment lacking both the N-terminal motor and the C-terminal tail domains, and (3) a tetrameric 378 kDa MW native "motorless" (a.k.a. "headless") fragment (Figure 1A). As expected, highly purified motorless KLP61F, like the full-length protein, displayed robust MT-bundling activity, whereas the purified stalk subfragment displayed no detectable bundling activity (Figure 2A), supporting the idea that KLP61F homotetramers must contain either N-terminal motor domains or C-terminal tail domains to be capable of bundling MTs [7].

To determine whether KLP61F has a preference for crosslinking MTs into either parallel or antiparallel bundles, polarity-marked MTs and purified KLP61F [7] (Figure 1A) were mixed for 1 min in assay buffer containing nucleotides, and they were subsequently introduced into a microscope chamber with an aminosilanized glass surface, which led to a fixation of the relative orientation of MTs upon attachment. After rinsing the sample, we counted the parallel and antiparallel MT bundles attached to the surface to determine their relative abundance (Figure 2B). In these assays, unlike the more routine bundling

*Correspondence: jmscholey@ucdavis.edu (J.M.S.), erwinp@nat.vu.nl (E.J.G.P.)

[4]These authors contributed equally to this work

[5]Present address: Department of Neuroscience, Erasmus Medical Center, 3015 GE Rotterdam, The Netherlands

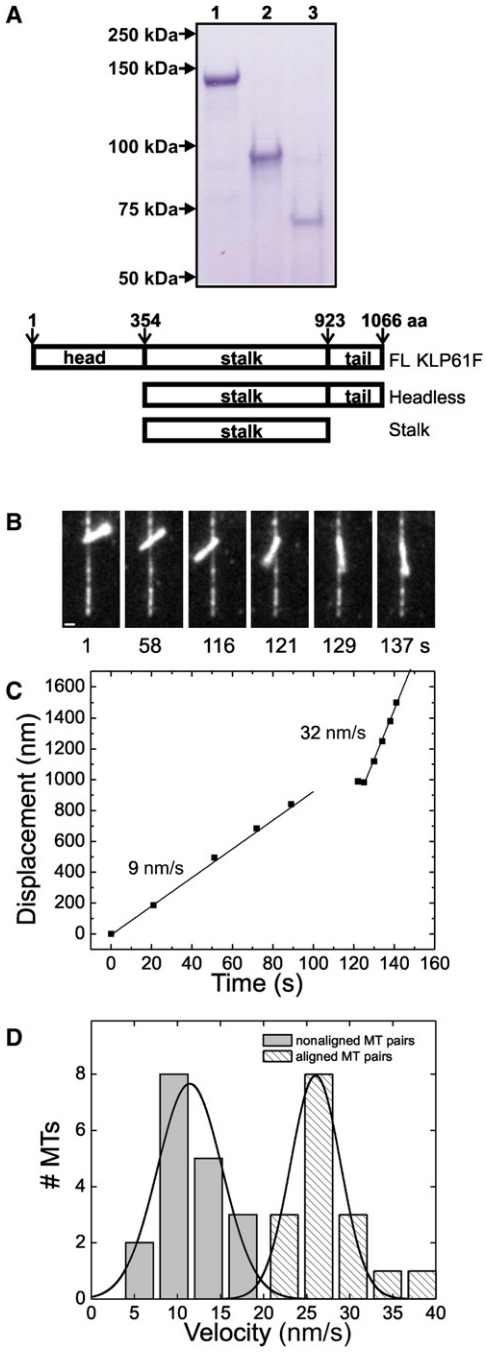

Figure 1. Purified KLP61F Can Crosslink and Slide Adjacent MTs

(A) Characterization of purified recombinant full-length (FL) KLP61F, headless KLP61F (lacking motor domains), and KLP61F stalk used in these studies. The Coomassie blue-stained SDS-polyacrylamide gel shows the purity of recombinant proteins after gel filtration (Superose 6 FPLC, GE Pharmacia). Lane 1 shows FL KLP61F, Lane 2 shows headless KLP61F (stalk + tail), and Lane 3 shows KLP61F stalk.

(B) Frames from a time-lapse recording showing a relatively short rhodamine-labeled MT sliding sideways (down and left) along a surface-attached Cy5-labeled MT. After 120 s, the sliding MT rotates and aligns with the immobilized MT. The two velocities now add, indicating antiparallel orientation. The scale bar represents 1 μm. See also Movies S1 and S2.

(C) Displacement of the hindmost interaction point of the rhodamine-labeled MT along the immobilized MT axis in (B) is plotted versus time. A linear fit reveals two sliding velocities.

(D) Histograms of velocities of all measured MTs in aligned and nonaligned configurations, shown together with Gaussian fits.

assays shown in Figure 2A, the relative concentration of KLP61F and MTs was optimized to generate bundles consisting of two MTs and not more.

We observed that, in saturating concentrations of the nonhydrolyzable ATP analog AMPPNP, equal numbers of parallel and antiparallel MT pairs were formed (Figure 2C). We reason that this occurred because AMPPNP facilitates the strong binding of KLP61F motor domains to the MT tracks, immediately locking them in place in a tight binding state. In other words, AMPPNP freezes the on and off kinetics of the motors and will not allow potential differences in binding affinity of either the motor domains or the binding domains in the tails between antiparallel and parallel MTs to establish a preferred polarity pattern. The result further suggests that each individual KLP61F motor has considerable rotational flexibility (consistent with Figures 1B–1D) because the pairs of motor domains at opposite ends of the stalk domain must be capable of rotating by 180° in order to crosslink MTs oriented in either parallel or antiparallel configurations. It should also be noted that, even if the orientational preference of a single crosslink was small compared to thermal energies, several motors could still collectively cause a strong orientational bias over time if the crosslinking is transient.

In principle, the two sets of binding sites, on the motor domains and on the tails, could each cause an orientational bias, the bias could be equal or opposite, or just one set could cause the bias. We designed the following experiments to differentiate between the various scenarios. The existence of a bias implies a certain degree of mechanical torsional stiffness in the tetramers. Note that a bias caused by only one set of binding sites allows one to roughly localize flexibility in the molecule. To avoid the initial "orientation quench" caused by AMPPNP on the motor domains, which appears to lock KLP61F-MT complexes in a random initial tight binding configuration, we modified the assay. We first incubated MTs and KLP61F in the presence of ATP for 1 min to allow the system to equilibrate. This time is appropriate because it exceeds the residence time of individual kinesin-5 motors on MTs but is short enough to prevent sliding to the end of travel, whereupon kinesin-5 reaches the ends of "sorted" MTs. When this is allowed to occur, complicating events (e.g., "snap-backs" of dangling MTs, et cetera) can introduce artifacts into the assays (discussed in [4]). After incubation, the crosslinked MTs were attached to the glass surface, and AMPPNP was flushed in to lock the KLP61F motors in an immotile state. Under these conditions, we observed three times more antiparallel MT pairs than parallel ones, indicating that the full-length KLP61F has a preference for generating antiparallel MT pairs in the presence of ATP (Figure 2C).

Earlier studies had shown that the KLP61F homolog Eg5 can diffuse axially along the MT polymer lattice in the presence of adenosine diphosphate (ADP) [13]; this process presumably does not involve specific and strong binding states of the motor domains but probably depends on interactions with the C-terminal tail domains instead [7, 14]. To examine the MT-bundling behavior of KLP61F in this "diffusive mode," in which the binding via the motor domains is likely switched off, we tested MT-MT crosslinking in the presence of KLP61F and ADP. We again observed three times more antiparallel than parallel MT crosslinking under these conditions. All results thus suggest that the tail binding sites are responsible for the bias. To entirely exclude the possiblity that the motor domains are required, we tested whether KLP61F's C-terminal MT-binding domains alone can cause the orientational preference of these kinesin-5 motors. We determined the orientation of MTs

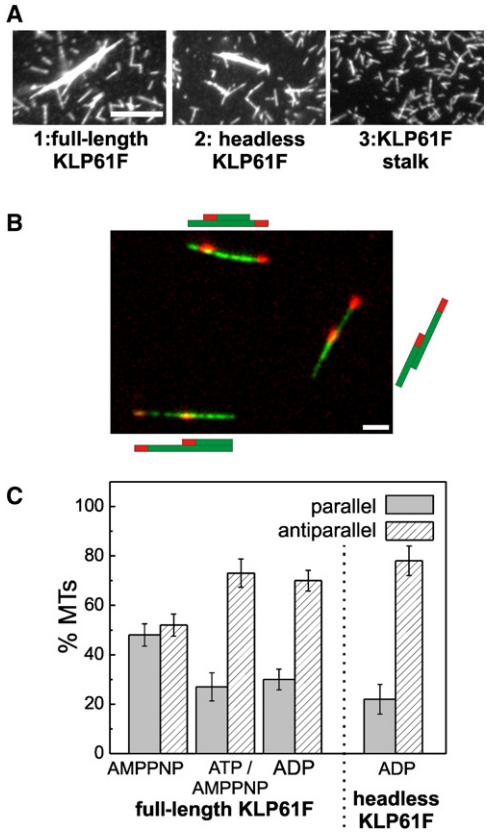

Figure 2. KLP61F Has a Preference for Crosslinking MTs into Antiparallel Orientations

(A) Pure FL KLP61F and motorless KLP61F, but not KLP61F stalk, can crosslink and bundle MTs in 1 mM ATP. Fluorescence microscopy shows that headless KLP61F and FL KLP61F have obvious bundling activity. KLP61F stalk without motor and tail domains, however, did not bundle MTs under the same conditions. The scale bar represents 10 μm.

(B) Image showing crosslinked pairs of polarity-marked MTs. The minus end of the MT is indicated in red, and the plus end is indicated in green. When two MTs are bundled, the fluorescence intensity doubles. On the basis of the relative fluorescence intensity and the location of the polarity marks, the orientation of crosslinking can be determined, as indicated. The white scale bar represents 2 μm.

(C) Histogram showing the orientation of MT crosslinking by FL KLP61F in the presence of AMPPNP (n = 124), ATP plus AMPPNP (n = 60), and ADP (n = 122), as well as by the motorless KLP61F (n = 49). The errors indicated were calculated from the propagation of the counting errors (square root of the number of counts in each category).

bundled by motorless constructs (which were already shown to bundle MTs [Figure 2A]) in the presence of ADP. We again observed three times more antiparallel than parallel MT bundles (Figure 2C). KLP61F thus has an approximately 3-fold preference for bundling antiparallel MTs over parallel ones. This preference is preserved when the motor domains are totally absent, as was the case for the motorless subfragment, or when they are switched off in a weakly and dynamically bound MT-binding state in the absence of ATP and in the presence of ADP.

Taken together, our results demonstrate that the homotetrameric kinesin-5 KLP61F, like its homolog, Eg5, can crosslink and slide MTs. Our findings further suggest that kinesin-5 motors display a preference for crosslinking MTs into antiparallel bundles. It may be reasonable to assume that the bipolar structure observed for *Drosophila* KLP61F [5] and the MT-MT sliding activity demonstrated for *Xenopus* Eg5 [4] are shared by all members of the kinesin-5 family. However, kinesin-5 motors appear to be deployed to play different roles in spindles from different systems [15–20], and these roles could be correlated with system-specific differences in the molecular architecture and mechanism of action of kinesin-5 motors. KLP61F is, to our knowledge, the first member of the kinesin-5 family explicitly shown to display both a bipolar ultrastructure [5] and MT-MT sliding activity (this report), both of which underlie the proposed kinesin-5-dependent "sliding filament" mechanism.

We do not know the molecular mechanism by which KLP61F preferentially crosslinks MTs into antiparallel orientations. This is a fascinating problem that merits further detailed analysis. The observation that tetramers of both ADP-bound full-length KLP61F and motorless KLP61F subfragments preferentially crosslink MTs into antiparallel orientations shows that the mechanochemical activity of the motor domains is not essential for the antiparallel polarity preference. In this context, it is interesting to note that MT crosslinking is also brought about by the nonmotor MT-binding protein Ase1p, which displays a similar antiparallel orientation preference [21]. Note that the antiparallel MT orientation preference of motorless KLP61F suggests that the C-terminal tail domains may control the polarity preference of full-length KLP61F, but we cannot exclude the possibility that active KLP61F motor domains (in contrast to those trapped in the presence of AMPPNP) could contribute as well. We also note that the tail domains contain the cyclin-dependent kinase (cdk)-dependent phosphorylatable bimC box, which may target kinesin-5 to spindle MTs [12, 22], so it is tempting to speculate that the phosphorylation state of the bimC box influences the polarity preference of kinesin-5. For addressing the above issues, detailed structure-function studies of the MT-crosslinking polarity preference of headless and tailless, phosphorylated and nonphosphorylated KLP61F constructs are planned.

On the basis of the results of the relative sliding experiments (Figure 1), together with the absence of any MT-crosslinking orientation preference in the presence of AMPPNP (Figure 2), it is apparent that full-length KLP61F is flexible enough to crosslink MTs in any orientation. However, to explain the orientation preference that is observed in the presence of ADP and ATP, we imagine that some part of the tetramer must have sufficient torsional rigidity to form and maintain the antiparallel MT orientation. This apparent contradiction is resolved if one assumes that the stalk between the opposing tail domains is relatively rigid, that the C-terminal tail domains specifically interact with a MT, resulting in an antiparallel orientation preference, and that the flexibility of the motor domains resides in the neck and/or neck linker. An improved understanding of the torsional rigidity of different domains of the KLP61F homotetramer would therefore be illuminating.

What are the implications of kinesin-5's antiparallel polarity preference for the mechanism of mitosis? At present, there is considerable interest in the mechanisms for establishing MT polarity patterns within mitotic spindles and in other MT-based structures, such as axons and dendrites [21, 23, 24]. In astral mitotic spindles, such as those in the early *Drosophila* embryo, spindle MTs are organized into two overlapping radial arrays, with their minus ends located at the centrosomes and their plus ends facing the equator of the spindle [12]. Consequently, MTs around and near the centrosomes are oriented parallel, whereas MTs overlapping with their plus ends at the equator are likely to encounter antiparallel neighbors. These

antiparallel pairs are crucial for generating forces between the spindle poles. In some spindles, such as *Drosophila* embryo mitotic spindles, motor-dependent crosslinking and relative sliding of antiparallel MTs at the spindle equator is thought to underlie poleward flux within interpolar MT (ipMT) bundles and pole-pole separation during anaphase spindle elongation [15, 25–28]. It is plausible that antiparallel ipMT-MT crosslinking and sliding by kinesin-5, acting in concert with nonmotor MT-associated proteins and with nucleated-MT assembly around centrosomes and chromosomes, could play significant roles in establishing the MT polarity patterns found in spindles [21, 24, 29].

To our knowledge, the specific MT orientation preference of KLP61F motors is so far unique among mitotic sliding motors. The fact that purified kinesin-5 motors all appear to be slow, plus-end-directed bipolar homotetramers capable of crosslinking adjacent MTs is consistent with the idea that kinesin-5 homotetramers serve as dynamic MT-MT crosslinks that both bundle parallel MTs and drive antiparallel MT sliding [12, 25, 30] and that this is their main contribution to mitotic spindle morphogenesis and function. Our results suggest that in the *Drosophila* embryo, KLP61F could initially bind and crosslink MTs of either polarity throughout the spindle, thereby "zipping" together parallel MTs to form MT bundles. This might be aided by an additional "stickiness" caused by the tail domains. Then via on and off kinetics or after moving toward crosslinked MT plus ends, the antiparallel preference mediated by the tails would cause KLP61F to accumulate in the overlap region of antiparallel ipMTs at the spindle equator to efficiently slide them apart, thereby contributing to poleward flux and spindle elongation [12, 15].

Experimental Procedures

Protein Preparation and Characterization

Three different constructs corresponding to full-length KLP61F, headless KLP61F, and KLP61F stalk were generated as described previously [7]. After verification by sequencing, the recombinant constructs were used for generating recombinant baculovirus (Invitrogen Baculovirus Expression System). Amplified virus was used for infecting sf9 cells. The proteins were purified from cell lysates with a Ni-NTA affinity column (QIAGEN), followed by superose 6 gel-filtration fast protein liquid chromatography (FPLC; GE Pharmacia). Tubulin and polarity-marked MTs were prepared as described before [4, 7, 21]. In short, rhodamine-labeled tubulin was purchased from Cytoskeleton Inc. Fluorescent (and biotinylated) MTs were polymerized from a mixture of 0.1 μM Cy5- or rhodamine-labeled tubulin (0.8 μM biotin-labeled tubulin) and 10 μM unmodified tubulin in the presence of 1 mM GpCpp (Jena Bioscience) and 2 mM DTT at 35°C for 25 min. For constructing polarity-marked MTs, MTs were further incubated in the presence of a mixture of 0.4 μM NEM-tubulin, 0.1 μM rhodamine-labeled tubulin, and 0.4 μM unmodified tubulin for 30 min. After stabilization with 10 μM paclitaxel (Sigma-Aldrich), MTs were centrifuged through a glycerol cushion (50% [v/v]) with a Beckman Coulter Airfuge Ultracentrifuge (operated at at a pressure of 25 psig) for removal of free tubulin, and the MTs were subsequently resuspended.

MT-Bundling Assay and Hydrodynamic Assays

Both assays were performed exactly as described previously for purified full-length KLP61F [7]. In the case of KLP61F subfragments, instead of partially purified proteins from a Ni-NTA affinity column, pure motorless subfragments and stalk subfragments were used after FPLC purification. From hydrodynamic assays, the full-length KLP61F homotetramer had Stokes radius (Rs) = 16.7 nm, sedimentation coefficient (S value) = 7.4 S, and native MW = 520 kDa; the motorless KLP61F homotetramer (K354–1066) had Rs = 16.4 nm, S value = 5.5 S, and native MW = 378 kDa; and the KLP61F stalk homotetramer (K354–923) had Rs = 13.3 nm, S value = 4.9 S, and native MW = 272 kDa.

Fluorescence Microscopy

MT sliding and orientation experiments were performed at 21°C with a custom-built wide-field fluorescence microscope described previously [4, 14], with a 100× Nikon S-Fluor objective (NA = 1.3). For simultaneous observation of rhodamine and Cy5, the sample was simultaneously illuminated with 635 nm (Power Technology Inc., IQ1C10[LD1338]G3H5) and 532 nm (Coherent, Compass 215M-20) laser light. The emission was first filtered with a triple band-pass filter (Z488/532/633M, Chroma), then separated with a dichroic beam splitter (565DCXR, Chroma), and finally redirected onto the tube lens at slightly different angles, resulting in two separate images on the camera chip (Micromax, Roper Scientific). Images were taken at a frame rate of 1 frame/s, and typical laser intensities used were 10 W/cm^2.

Relative MT Sliding Assays

Tubulin and polarity-marked MTs were prepared as described above and before [4]. Coverslips were treated with dimethyl-dichlorosilane [4], and chambers were prepared by attaching the coverslips to microscope slides with double-stick tape. Chambers were incubated for 5 min with BSA-biotin (Sigma-Aldrich, 0.1 mg/ml) in PEM80 (80 mM K_2PIPES, 1 mM EGTA, 2 mM $MgCl_2$ [pH 6.8], set with HCl), washed with buffer, and incubated for 5 min with streptavidin (Biochemika, 0.1 mg/ml). The surface was blocked by incubation with a watery solution of Pluronic F108 (0.2% [w/v], BASF) for 5 min. Next, the chambers were incubated with biotinylated Cy5-labeled MTs (5 min). After rinsing with buffer, the chambers were flushed with 1 nM KLP61F, 2 mM ATP, and rhodamine-labeled MTs in motility buffer (PEM80 [pH 6.8], 10 μM paclitaxel, 0.2% Pluronic F108, 4 mM DTT, and 25 mM glucose, 20 μg/ml glucose oxidase, and 35 μg/ml catalase).

Assays to Determine the Orientation of MTs Bundled by KLP61F

In order to determine the crosslinking preference of KP61F, we used coverslips that were positively charged by silanization with 0.1% (V/V) DETA [3-(2-(2-aminoethylamino)ethyl-amino)propyl-trimethoxysilane, Aldrich] in water (incubated for 10 min, subsequently washed in water). Sample chambers were incubated with a mixture of polarity-marked MTs, 20 nM KLP61F, and 2 mM nucleotide (AMPPNP, ATP plus AMPPNP, or ADP) in motility buffer. Fluorescent images were taken, and for all observed bundles consisting of two MTs of which the polarity could be unambiguously assigned, the relative orientation was determined. For each experiment, control experiments without KLP61F and with KLP61F stalk subfragments were performed for excluding the possibility that MT bundling occurred nonspecifically.

Supplemental Data

Supplemental Data include two movies and can be found with this article online at http://www.current-biology.com/supplemental/S0960-9822(08)01395-X.

Acknowledgments

This work is part of the research program of the Stichting voor Fundamenteel Onderzoek der Materie (FOM), which is financially supported by the Nederlandse Organisatie voor Wetenschappelijk Onderzoek (NWO). L.K. and E.P. were supported by a VIDI fellowship to E.P. from the Research Council for Earth and Life Sciences (ALW). L.T. and J.M.S were supported by National Institutes of Health grant GM55507 to J.M.S. C.F.S. was supported by the German Research Foundation (DFG) Center for the Molecular Physiology of the Brain (CMPB).

Received: September 9, 2008
Revised: October 6, 2008
Accepted: October 8, 2008
Published online: December 4, 2008

References

1. Brust-Mascher, I., and Scholey, J.M. (2007). Mitotic spindle dynamics in Drosophila. Int. Rev. Cytol. *259*, 139–172.
2. Walczak, C.E., and Heald, R. (2008). Mechanisms of mitotic spindle assembly and function. Int. Rev. Cytol. *265*, 111–158.
3. Cole, D.G., Saxton, W.M., Sheehan, K.B., and Scholey, J.M. (1994). A "slow" homotetrameric kinesin-related motor protein purified from Drosophila embryos. J. Biol. Chem. *269*, 22913–22916.
4. Kapitein, L.C., Peterman, E.J., Kwok, B.H., Kim, J.H., Kapoor, T.M., and Schmidt, C.F. (2005). The bipolar mitotic kinesin Eg5 moves on both microtubules that it crosslinks. Nature *435*, 114–118.

5. Kashina, A.S., Baskin, R.J., Cole, D.G., Wedaman, K.P., Saxton, W.M., and Scholey, J.M. (1996). A bipolar kinesin. Nature *379*, 270–272.
6. Sawin, K.E., LeGuellec, K., Philippe, M., and Mitchison, T.J. (1992). Mitotic spindle organization by a plus-end-directed microtubule motor. Nature *359*, 540–543.
7. Tao, L., Mogilner, A., Civelekoglu-Scholey, G., Wollman, R., Evans, J., Stahlberg, H., and Scholey, J.M. (2006). A homotetrameric kinesin-5, KLP61F, bundles microtubules and antagonizes Ncd in motility assays. Curr. Biol. *16*, 2293–2302.
8. Hildebrandt, E.R., Gheber, L., Kingsbury, T., and Hoyt, M.A. (2006). Homotetrameric form of Cin8p, a Saccharomyces cerevisiae kinesin-5 motor, is essential for its in vivo function. J. Biol. Chem. *281*, 26004–26013.
9. Valentine, M.T., Fordyce, P.M., and Block, S.M. (2006). Eg5 steps it up! Cell Div. *1*, 31.
10. Civelekoglu-Scholey, G., and Scholey, J.M. (2007). Mitotic motors: Kinesin-5 takes a brake. Curr. Biol. *17*, R544–R547.
11. Cottingham, F.R., Gheber, L., Miller, D.L., and Hoyt, M.A. (1999). Novel roles for saccharomyces cerevisiae mitotic spindle motors. J. Cell Biol. *147*, 335–350.
12. Sharp, D.J., McDonald, K.L., Brown, H.M., Matthies, H.J., Walczak, C., Vale, R.D., Mitchison, T.J., and Scholey, J.M. (1999). The bipolar kinesin, KLP61F, cross-links microtubules within interpolar microtubule bundles of Drosophila embryonic mitotic spindles. J. Cell Biol. *144*, 125–138.
13. Kwok, B.H., Kapitein, L.C., Kim, J.H., Peterman, E.J., Schmidt, C.F., and Kapoor, T.M. (2006). Allosteric inhibition of kinesin-5 modulates its processive directional motility. Nat. Chem. Biol. *2*, 480–485.
14. Kapitein, L.C., Kwok, B.H., Weinger, J.S., Schmidt, C.F., Kapoor, T.M., and Peterman, E.J. (2008). Microtubule cross-linking triggers the directional motility of kinesin-5. J. Cell Biol. *182*, 421–428.
15. Brust-Mascher, I., Civelekoglu-Scholey, G., Kwon, M., Mogilner, A., and Scholey, J.M. (2004). Model for anaphase B: Role of three mitotic motors in a switch from poleward flux to spindle elongation. Proc. Natl. Acad. Sci. USA *101*, 15938–15943.
16. Goshima, G., and Vale, R.D. (2003). The roles of microtubule-based motor proteins in mitosis: Comprehensive RNAi analysis in the Drosophila S2 cell line. J. Cell Biol. *162*, 1003–1016.
17. Heck, M.M., Pereira, A., Pesavento, P., Yannoni, Y., Spradling, A.C., and Goldstein, L.S. (1993). The kinesin-like protein KLP61F is essential for mitosis in Drosophila. J. Cell Biol. *123*, 665–679.
18. Miyamoto, D.T., Perlman, Z.E., Burbank, K.S., Groen, A.C., and Mitchison, T.J. (2004). The kinesin Eg5 drives poleward microtubule flux in Xenopus laevis egg extract spindles. J. Cell Biol. *167*, 813–818.
19. Saunders, A.M., Powers, J., Strome, S., and Saxton, W.M. (2007). Kinesin-5 acts as a brake in anaphase spindle elongation. Curr. Biol. *17*, R453–R454.
20. Saunders, W.S., and Hoyt, M.A. (1992). Kinesin-related proteins required for structural integrity of the mitotic spindle. Cell *70*, 451–458.
21. Janson, M.E., Loughlin, R., Loiodice, I., Fu, C., Brunner, D., Nedelec, F.J., and Tran, P.T. (2007). Crosslinkers and motors organize dynamic microtubules to form stable bipolar arrays in fission yeast. Cell *128*, 357–368.
22. Sawin, K.E., and Mitchison, T.J. (1995). Mutations in the kinesin-like protein Eg5 disrupting localization to the mitotic spindle. Proc. Natl. Acad. Sci. USA *92*, 4289–4293.
23. Baas, P.W., Deitch, J.S., Black, M.M., and Banker, G.A. (1988). Polarity orientation of microtubules in hippocampal neurons: Uniformity in the axon and nonuniformity in the dendrite. Proc. Natl. Acad. Sci. USA *85*, 8335–8339.
24. Channels, W.E., Nedelec, F.J., Zheng, Y., and Iglesias, P.A. (2008). Spatial regulation improves antiparallel microtubule overlap during mitotic spindle assembly. Biophys. J. *94*, 2598–2609.
25. McIntosh, J.R., Hepler, P.K., and Van Wie, D.G. (1969). Model for mitosis. Nature *224*, 659–663.
26. McIntosh, J.R., McDonald, K.L., Edwards, M.K., and Ross, B.M. (1979). Three-dimensional structure of the central mitotic spindle of Diatoma vulgare. J. Cell Biol. *83*, 428–442.
27. Saxton, W.M., and McIntosh, J.R. (1987). Interzone microtubule behavior in late anaphase and telophase spindles. J. Cell Biol. *105*, 875–886.
28. Straight, A.F., Sedat, J.W., and Murray, A.W. (1998). Time-lapse microscopy reveals unique roles for kinesins during anaphase in budding yeast. J. Cell Biol. *143*, 687–694.
29. Walczak, C.E., Vernos, I., Mitchison, T.J., Karsenti, E., and Heald, R. (1998). A model for the proposed roles of different microtubule-based motor proteins in establishing spindle bipolarity. Curr. Biol. *8*, 903–913.
30. Uteng, M., Hentrich, C., Miura, K., Bieling, P., and Surrey, T. (2008). Poleward transport of Eg5 by dynein-dynactin in Xenopus laevis egg extract spindles. J. Cell Biol. *182*, 715–726.